

# Robust Control Design of Wheeled Inverted Pendulum Assistant Robot

Magdi S. Mahmoud and Mohammad T. Nasir

**Abstract**—This paper examines the design concept and mobile control strategy of the human assistant robot I-PENTAR (inverted pendulum type assistant robot). The motion equation is derived considering the non-holonomic constraint of the two-wheeled mobile robot. Different optimal control approaches are applied to a linearized model of I-PENTAR. These include linear quadratic regulator (LQR), linear quadratic Gaussian control (LQG),  $H_2$  control and  $H_\infty$  control. Simulation is performed for all the approaches yielding good performance results.

**Index Terms**—I-PENTAR robot, linear quadratic regulator (LQR) control design, model predictive control (MPC), observer-based feedback control, robust  $H_\infty$  control.

## I. INTRODUCTION

RECENTLY, robots have been used in many applications including industry and human ordinary life. Robots can make the human life easier by doing the dangerous works such as working in a toxic environment or by doing the hard works such as carrying heavy objects. And also robots can add more precision and repeatability in many tasks such as welding and assembly tasks.

Inverted pendulum type assistant robot (I-PENTAR) is a humanoid type robot which consists of a body with a waist joint, two degrees of freedom (DOF) arms designed for safety, and a wheeled inverted pendulum mobile platform, see Fig. 1. Although the arms are designed at low-power and lightweight for safety, it is capable to perform high power tasks by utilizing its self-weight, which is the feature of a wheeled inverted pendulum mobile platform. I-PENTAR is modeled as a three dimensional robot; with controls of inclination angle, horizontal position, and steering angle to achieve high mobile capability. The motion equation is derived considering the non-holonomic constraint of the two-wheeled mobile robot. Wheeled inverted pendulum is considered highly unstable robot, thus achieving the stability is the key that controller approaches are designed for.

Two wheeled mobile robot balancing controller has been tackled as a linearized model [1] or as a nonlinear model

Manuscript received May 20, 2016; accepted February 6, 2017. This work was supported by the Deanship of Scientific Research (DSR) at the King Fahd University of Petroleum and Minerals (KFUPM) (141048). Recommended by Associate Editor Zhijun Li. (*Corresponding author: Magdi S. Mahmoud*)

Citation: M. S. Mahmoud and M. T. Nasir, “Robust control design of wheeled inverted pendulum assistant robot,” *IEEE/CAA J. of Autom. Sinica*, vol. 4, no.4, pp. 628–638, Oct. 2017.

M. S. Mahmoud and M. T. Nasir are with the Systems Engineering Department, King Fahd University of Petroleum and Minerals, Dhahran 31261, Saudi Arabia (e-mail: msmahmoud@kfupm.edu.sa; g201207520@kfupm.edu.sa).

Color versions of one or more of the figures in this paper are available online at <http://ieeexplore.ieee.org>.

Digital Object Identifier 10.1109/JAS.2017.7510613

[2]. Another work tackled the nonlinear disturbance [3] by developing an nonlinear observer. In [4] a two wheeled mobile robot is designed and a comparison between the linearized and nonlinear model is done experimentally. An MPC (model predictive control) controller presented by [5] was designed to maintain the robot at balance.

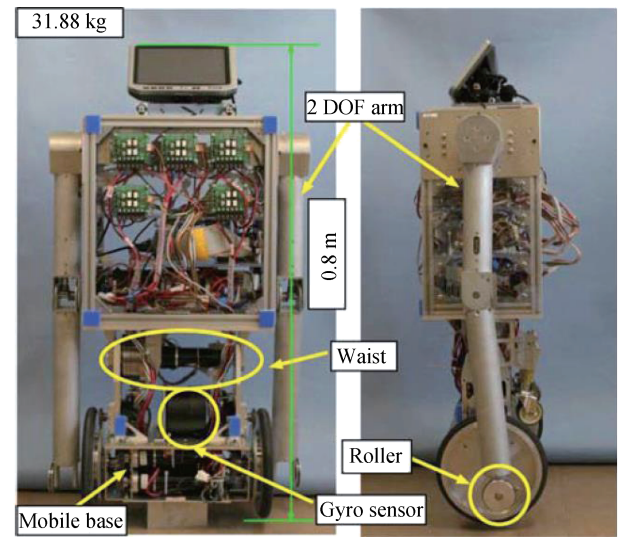


Fig. 1. I-PENTAR wheeled inverted pendulum robot.

One of the key challenges in using robots is its uncertainty. This uncertainty can be in the robot parameters such as its mass, inertia and the friction factors or in the sensors readings such as the robot speed and inclination angle. And also uncertainty can be in the working area such as the carried object mass, inertia and size. The challenge is how to increase the performance of such robots with the existence of this uncertainty. The development of more robust and fast controller algorithms can tackle uncertainty.

Wheeled inverted pendulum is considered highly unstable robot, thus achieving the stability with existence of uncertainty is the key that controller approaches are particularly designed for. A recently identified technique for overcoming the complications inherent in wheeled inverted pendulum (WIP) systems is conveniently presented in [6].

The parametric and functional uncertainties were tackled with fuzzy control approach by [7], and with neural network approach by [8]. A model based robust sliding mode controller was proposed by [9]. In [10], a reference model for the yaw and tilt angle of the wheeled inverted pendulum is derived using the linear quadratic regulator (LQR) optimization to guarantee motion tracking. The accurate trajectory tracking control of a wheeled mobile robot was studied in [11] based

on the slip model prediction. Trajectory tracking control of the inertia wheel pendulum was treated in [12] using an uncertain model. A backstepping-based adaptive control is designed in [13] to achieve output tracking for the wheeled inverted pendulum and similarly an adaptive integral backstepping controller is developed in [14] to stabilize the body angle. Design aspects for wheeled inverted pendulum (WIP) platforms were examined in [15] to investigate the effect of design choices on the balancing performance.

In this paper, we build upon the results of [9]–[17] and extend them further. We consider the human assistant robot I-PENTAR and generate an appropriate linearized model. Then, we develop and establish complete control design results based on four distinct approaches:

- 1) Linear quadratic regulator (LQR) design, for which we establish a linear matrix inequality (LMI) formalism yielding a static state-feedback gain.

- 2) Linear quadratic Gaussian (LQG) design, for which we examine an observer-based feedback scheme.

- 3)  $H_2$  control design, for which we establish an LMI formalism based on the  $H_2$ -norm condition and yielding a dynamic-feedback structure and

- 4)  $H_\infty$  control design, for which we establish an LMI formalism based on the  $H_\infty$ -norm condition and yielding a dynamic-feedback structure.

The contributions of our work are summarized below:

- 1) The analytical results are derived in systematic and unique way thereby leading to improved techniques over the techniques in the literature.

- 2) Equal attention is paid to the nominal and uncertain representation of the human assistant robot I-PENTAR.

- 3) All the design procedures are conveniently cast into the format of feasibility problem over linear matrix inequalities (LMIs). By this way, effective computational methods are established yielding guaranteed quality solution.

- 4) Simulation studies are performed for all the approaches yielding good performance results.

- 5) Experimental results for the I-PENTAR during upright balancing are presented.

*Lemma 1* [18]: Given appropriately dimensioned matrices  $\Sigma_1, \Sigma_2, \Sigma_3$  with  $\Sigma_1 = \Sigma_1^t$ . Then,

$$\Sigma_1 + \Sigma_3 \Sigma_2 + \Sigma_2^t \Sigma_3^t < 0 \quad (1)$$

holds if for some matrix  $W > 0$

$$\Sigma_1 + \Sigma_3 W^{-1} \Sigma_3^t + \Sigma_2^t W \Sigma_2 < 0. \quad (2)$$

## II. INVERTED PENDULUM-TYPE ASSISTANT ROBOT

Fig. 1 shows the case study of I-PENTAR, which consists of two arms each with one elbow which can be used to maintain stability of the robot and two gyro-sensors to define the acceleration and the inclination angle relative to the flat surface of the earth. Two wheels are for movements in two degrees of freedom.

A model of pendulum robot is built on two dimensional models (linear position of  $x, z$  coordinates) with steering angle created from rotation and inclination angle caused by linear movements, see Fig. 2. The origin of vehicle coordinates

$\Sigma_\omega$  is located at the midpoint on the line that connects the axis of the two wheels, and the origin of the body coordinates  $\Sigma_b$  coincides with the  $\Sigma_u$ . The angle between  $z_b$  and  $z_v$  represents the inclination angle of the body  $\psi$ , and the angle between  $x_v$  and  $x_o$  axis of the global coordinates represents the steering angle  $\phi$ . In all the coordinates, counter-clock wise (CCW) direction is positive.

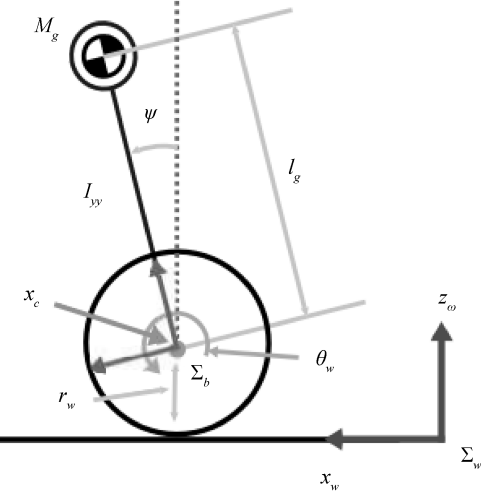


Fig. 2. Two DOF wheeled inverted pendulum robot.

Following the work of [1]–[17], the nonlinear robot model  $\dot{\mathbf{x}} = f(\mathbf{x}, \mathbf{u}, \mathbf{w})$  can be conveniently cast into the uncertain linearized model:

$$\begin{aligned} \dot{\mathbf{x}}(t) &= (A + \delta A)\mathbf{x}(t) + (B + \delta B)\mathbf{u}(t) + \Gamma\mathbf{w}(t) \\ &= A_\delta\mathbf{x}(t) + B_\delta\mathbf{u}(t) + \Gamma\mathbf{w}(t) \\ \mathbf{z}(t) &= G\mathbf{x}(t) + D\mathbf{u}(t) + \Phi\mathbf{w}(t) \\ \mathbf{y}(t) &= C\mathbf{x}(t) + \Psi\mathbf{w}(t) \end{aligned} \quad (3)$$

where  $\mathbf{x}(t) \in \mathbb{R}^n$ ,  $\mathbf{u}(t) \in \mathbb{R}^m$ ,  $\mathbf{y}(t) \in \mathbb{R}^p$  are the state, the control input and the measured output vectors and  $\delta A$ ,  $\delta B$  accounts for the parametric uncertainties and for convenience they are expressed as

$$[\delta A \ \delta B] = H_a F [E_a \ E_c], \quad F^T F \leq I. \quad (4)$$

The state variables are  $x_v, \varphi, \psi, \dot{x}_v, \dot{\varphi}, \dot{\psi}$  where  $x_v$  is the linear position of the vehicle (m),  $\varphi$  is the inclination angle of center of gravity (CoG) in (rad) and  $\psi$  is the steering angle of the vehicle in (rad). The matrices  $H_a$ ,  $E_a$ ,  $E_c$  are selected to reflect the amount of deviation in model parameters from nominal levels. Observe that modeling errors and/or parametric uncertainties are incorporated in (3) to reflect some practicality in replacing the nonlinear model  $\dot{\mathbf{x}} = f(\mathbf{x}, \mathbf{u}, \mathbf{w})$ . By quasi-linearization at appropriate operating point [1]–[3], the matrices  $A$ ,  $B$ ,  $C$  are given by:

$$\begin{aligned} A &= \begin{bmatrix} 0 & I \\ A_1 & A_2 \end{bmatrix}, \quad B = \begin{bmatrix} 0 \\ B_1 \end{bmatrix}, \quad C = \begin{bmatrix} I & 0 \end{bmatrix} \\ A_1 &= \begin{bmatrix} 0 & 0 & a_{43} \\ 0 & 0 & 0 \\ 0 & 0 & a_{63} \end{bmatrix}, \quad A_2 = \begin{bmatrix} a_{44} & a_{45} & a_{46} \\ a_{54} & a_{55} & a_{56} \\ a_{64} & a_{65} & a_{66} \end{bmatrix} \\ B_1 &= \begin{bmatrix} b_1 & b_2 \\ b_3 & b_4 \\ b_5 & b_6 \end{bmatrix}. \end{aligned} \quad (5)$$

The numerical values of the parameters are presented in Table I.

TABLE I  
NUMERICAL DATA

Parameter	Value
$M_g$	25.26 kg
$m_g$	125 kg
$\ell_g$	0.4005 m
$b$	0.16 m
$r_w$	0.1 m
$I_g$	1.408 kg· m <sup>2</sup>
$I_{wa}$	0.01475 kg· m <sup>2</sup>
$I_{wd}$	0.0073 kg· m <sup>2</sup>
$I_{ra}$	0
$I_{rd}$	0
$\gamma$	1
$c_r$	0.1 Nm· s/rad
$c_\ell$	0.1 Nm· s/rad
$G$	9.81

$$\begin{aligned}
 a_{43} &= \frac{M_g^2 \ell_g^2 r_w^2 G}{V_1}, \quad a_{44} = \frac{w_1 c_1}{V_1}, \quad a_{55} = \frac{-b^2 c_1}{V_2} \\
 a_{45} &= \frac{w_1 c_1}{V_1}, \quad a_{46} = \frac{-r_w w_1 c_1}{V_1}, \quad a_{54} = \frac{-bc_2}{V_2} \\
 a_{56} &= \frac{br_w w_1 c_2}{V_2}, \quad a_{64} = \frac{-w_2 c_1}{r_w V_1}, \quad a_{65} = \frac{-bw_2 c_2}{r_w V_1} \\
 a_{63} &= \frac{(M_g r_w^2 + 2m_w r_w^2 + 2(I_{wa} + \gamma I_{ra})) M_g I_g G}{V_1} \\
 b_1 &= b_2 = \frac{-r_w w_1}{V_1}, \quad b_3 = -b_4 = \frac{-r_w b}{V_2} \\
 b_5 &= b_6 = \frac{w_2}{V_1}, \quad a_{66} = \frac{-w_2 c_1}{V_1} \\
 V_1 &= I_{zz} r_w^2 + 2(I_{wd} + I_{rd}) + 2m_w r_w^2 b^2 \\
 &\quad + 2(I_{wa} + \gamma^2 I_{ra}) b^2 \\
 w_1 &= M_g \ell_g^2 + I_{yy} + M_g \ell_g r_w \\
 w_2 &= M_g \ell_g r_w + M_g r_w^2 + 2m_w r_w^2 + 2(I_{wa} + \gamma^2 I_{ra})
 \end{aligned}$$

### III. NOMINAL CONTROL DESIGN

In control system terminology, the problem under consideration is that of determining feedback controller that makes system (3) stable over a wide range of operation while achieving a prescribed performance measure. Next, we provide design techniques to achieve this goal.

#### A. LMI-based LQR

With focus on the linear-quadratic regulator (LQR) design with  $w(t) \equiv 0$ , the associated quadratic cost function [19] is

$$J = \int_0^\infty [\mathbf{y}^T(t) Q \mathbf{y}(t) + \mathbf{u}^T(t) R \mathbf{u}(t)] dt \quad (6)$$

where  $Q > 0$ ,  $R > 0$  are output error and control weighting matrices, which are selected in the course of simulation by observing several sets of criteria of the closed loop-system.

*Assumption 1:* System (3) possesses the following properties:

- 1) All the states  $\mathbf{x}(t)$  are available for feedback.
- 2) The system is stabilizable which means that all of its unstable modes are controllable.
- 3) The system is detectable having all its unstable modes observable.

In what follows, we present an LMI-based formulation to the LQ control of system (3) while minimizing the quadratic cost (6) for all admissible uncertainties  $F^T F \leq I$ . We proceed to determine a linear optimal state-feedback control  $\mathbf{u} = L \mathbf{x}$  that achieves this goal.

*Assumption 2:* There exists a Lyapunov functional  $V(\mathbf{x})$  which has the properties:

- 1)  $V(\mathbf{x}) = \mathbf{x}^T P \mathbf{x}$ ,  $P > 0$ ,
- 2) There exists  $\gamma_+ > 0$  such that  $\mathbf{x}_o^T P \mathbf{x}_o \leq \gamma_+$ .
- 3)  $\dot{V}(\mathbf{x}) \leq -[\mathbf{x}^T C^T Q C \mathbf{x} + \mathbf{u}^T R \mathbf{u}]$ .

Consider system (3) with linear control  $\mathbf{u} = L \mathbf{x}$ . The following theorem provides an LMI-based LQR design:

*Theorem 1:* Given matrices  $Q > 0$ ,  $R > 0$  and scalar  $\varepsilon > 0$ , system (3) with  $w(t) \equiv 0$  and the LQR control  $\mathbf{u} = L \mathbf{x}$  is robustly asymptotically stable for all admissible uncertainties  $F^T F \leq I$  and  $J_\infty \leq V(\mathbf{x}_o)$  if there exist matrices  $S$ ,  $Y > 0$  such that

$$\begin{aligned}
 &\min_{\gamma_+, Y, S} \gamma_+ \text{ subject to} \\
 &\Xi = AY + BS + YA^T + S^T B^T \\
 &\Lambda = YE_a^T + S^T E_c^T \\
 &\left[ \begin{array}{ccccc} \Xi & YC^T Q & S^T R & H_a & \varepsilon \Lambda \\ * & -Q & 0 & 0 & 0 \\ * & * & -R & 0 & 0 \\ * & * & * & -\varepsilon I & 0 \\ * & * & * & * & -\varepsilon I \end{array} \right] \leq 0 \quad (7) \\
 &\left[ \begin{array}{cc} \gamma_+ & \mathbf{x}_o^T \\ * & Y \end{array} \right] \geq 0 \quad (8)
 \end{aligned}$$

has a feasible solution, then LQR gain matrix is  $L = SY^{-1}$ .

*Proof:* By Assumption (2), and using control  $\mathbf{u} = L \mathbf{x}$  in system (3), the inequality of the derivative of the Lyapunov functional, for all uncertainties  $F : F^T F \leq I$ , is expressed for all  $x$  as

$$\begin{aligned}
 &\mathbf{x}^T [P(A_\delta + B_\delta L) + (A_\delta + B_\delta L)^T P] \mathbf{x} \\
 &\leq -\mathbf{x}^T [C^T Q C + L^T R L] \mathbf{x}. \quad (9)
 \end{aligned}$$

Invoking Lemma 1 for some  $L$ ,  $P > 0$ ,  $\varepsilon > 0$  and recalling (4), inequality (9) is satisfied when

$$\begin{aligned}
 &P(A + BL) + (A + BL)^T P + [C^T Q C + L^T R L] \\
 &+ \varepsilon^{-1} P H_a H_a^T P + \varepsilon (E_a + E_c L)^T (E_a + E_c L) \leq 0. \quad (10)
 \end{aligned}$$

Alternatively, simple computations on (6) in view of Assumption 2 yields  $J_\infty \leq V(\mathbf{x}_o)$ . By minimizing the upper bound  $\gamma_+$  on the cost  $\mathbf{x}_o^T P \mathbf{x}_o$ , we obtain

$$\min_{\gamma_+, P, L} \gamma_+ \text{ subject to (10).} \quad (11)$$

To convexify the above problem, we first express (10) as

$$\begin{aligned}\Phi &= P(A + BL) + (A + BL)^T P \\ \Psi &= (E_a + E_c L) \\ \tilde{\Pi} &= \begin{bmatrix} \Phi & C^T Q & L^T R & PH_a & \varepsilon \Psi^T \\ * & -Q & 0 & 0 & 0 \\ * & * & -R & 0 & 0 \\ * & * & * & -\varepsilon I & 0 \\ * & * & * & * & -\varepsilon I \end{bmatrix} \leq 0.\end{aligned}\quad (12)$$

Pre- and post-multiply (12) by  $\text{diag}\{Y, I, I, I, I\}$  and using  $Y = P^{-1}$ ,  $S = LP^{-1}$  it yields (7). Additionally, the inequality bound of the Lyapunov functional can be expressed as

$$\begin{bmatrix} \gamma_+ & x_o^T \\ * & P^{-1} \end{bmatrix} \geq 0 \quad (13)$$

which can be manipulated to yield (8). When a feasible solution is attained, we get  $L = S Y^{-1}$ ,  $P = Y^{-1}$  as desired. ■

*Remark 1:* The LQR formulation considered above suffered from the drawback that the optimal control law  $u = Lx$  required the whole state  $x$  of the process to be measurable. A possible approach to overcome this difficulty is to construct an estimate  $\hat{x}$  of the state of the process based solely on the past values of the measured output  $y$  and control signal  $u$ , and then use  $u = L\hat{x}$ . This approach is usually known as certainty equivalence and leads to the architecture in Fig. 3.

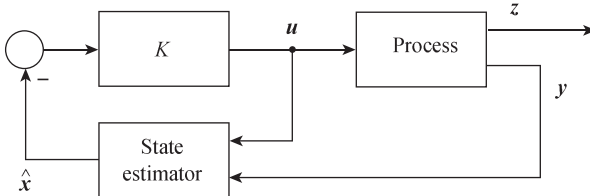


Fig. 3. Certainty equivalence controller.

### B. Deterministic Minimum-energy Estimation (MEE)

Consider system (3) with  $w(t) \neq 0$ . It is known that estimating the state  $x$  at some time  $t$  can be viewed as solving (3) for the unknown  $x$ , for given  $u(\tau)$ ,  $y(\tau)$ ,  $\tau \leq t$  for all admissible uncertainties  $F^T F \leq I$ . In practice, one seeks a minimum-energy estimation (MEE) which consists of finding the state trajectory

$$\begin{aligned}\dot{\bar{x}}(t) &= A_\delta \bar{x}(t) + B_\delta u(t) + \Gamma w(t) \\ y(t) &= C \bar{x}(t) + \Psi v(t)\end{aligned}\quad (14)$$

that is consistent with the past measured output  $y$  and control signal  $u$  for the least amount of noise  $w$ , measured by

$$\hat{J}_{\text{MEE}} = \int_{\infty}^t [w^T(\tau) Q w(\tau) + v^T(\tau) R v(\tau)] d\tau \quad (15)$$

where  $Q, R > 0$ . Once this trajectory has been found based on the data collected on the interval  $(\infty, t]$ , the minimum energy state estimate is simply the most recent value of  $\bar{x}$ ,

that is,  $\hat{x}(t) = \bar{x}(t)$ . It follows from [20] that by minimizing the quadratic cost

$$\begin{aligned}J_{\text{MEE}} &= \int_{\infty}^t [C \bar{x}(\tau) - y(\tau)]^T Q [C \bar{x}(\tau) - y(\tau)] \\ &\quad + v^T(\tau) R v(\tau) \} d\tau.\end{aligned}\quad (16)$$

The results are summarized by the following theorem:

*Theorem 2:* Assume that there exists a matrix  $0 < \mathcal{P}^T = \mathcal{P}$  solving the algebraic Riccati equation (ARE):

$$A_\delta \mathcal{P} + \mathcal{P} A_\delta + B_\delta R^{-1} B_\delta - \mathcal{P} C^T Q C \mathcal{P} \leq 0 \quad (17)$$

for all admissible uncertainties  $F^T F \leq I$ , then the MEE estimator for system (14) with criteria (15) is given by

$$\begin{aligned}\dot{\hat{x}}(t) &= [A - KC] \hat{x}(t) + Bu(t) + Ky(t) \\ K &= \mathcal{P} C^T Q.\end{aligned}\quad (18)$$

The MEE introduced before has a stochastic interpretation. Considering system (14) under the assumption that disturbance  $w$  and measurement noise  $v$  are uncorrelated zero-mean Gaussian white noise stochastic processes with covariance matrices:

$$\begin{aligned}\text{IE}[v(t)v^T(\tau)] &= \delta(t - \tau) R^{-1}, \quad R > 0 \\ \text{IE}[w(t)w^T(\tau)] &= \delta(t - \tau) Q^{-1}, \quad R > 0 \\ \text{IE}[v(t)w^T(\tau)] &= 0.\end{aligned}$$

Combining the LQR design, based on Theorem 1, with the MEE filter, based on Theorem 2, eventually generates the linear quadratic Gaussian (LQG) design. Indeed, the certainty equivalence principle guarantees that the designs are independent and hence could be computed in parallel.

### IV. DYNAMIC FEEDBACK CONTROL

In the sequel, we focus on the stabilizability problem with respect to the output-feedback controller

$$\begin{aligned}\dot{x}_c(t) &= A_c x_c(t) + B_c y(t) \\ u(t) &= C_c x_c(t) + D_c y(t)\end{aligned}\quad (19)$$

where  $x_c(t) \in \mathbb{R}^n$ . The feedback connection of the system (3) with  $w(t) \equiv 0$  and controller (19) yield a linear system described by

$$\begin{aligned}\dot{x}_s(t) &= A_s x_s(t) + B_s w(t) \\ z(t) &= C_s x_s(t) + D_s w(t)\end{aligned}\quad (20)$$

where

$$\begin{aligned}A_{s\delta} &= \begin{bmatrix} A_\delta + B_\delta D_c C & B_\delta C_c \\ B_c C & A_c \end{bmatrix}, \quad x_s(t) = \begin{bmatrix} x(t) \\ x_c(t) \end{bmatrix} \\ B_{s\delta} &= \begin{bmatrix} \Gamma + B_\delta D_c \Psi \\ B_c \Psi \end{bmatrix}, \quad C_s = [G + DD_c C \quad DC_c] \\ D_s &= \Phi + DD_c \Psi.\end{aligned}\quad (21)$$

Designing a dynamic controller for the system under consideration is approached via convex analysis. Suppose a Lyapunov function for the closed-loop system (20) is selected as

$$V(x_s) = x_s^T \mathcal{P} x_s(t), \quad 0 < \mathcal{P}^T = \mathcal{P} \in \mathbb{R}^{8 \times 8}. \quad (22)$$

Along the solutions of the closed-loop system (20) with  $w(t) \equiv 0$ , we obtain

$$\begin{aligned}\dot{V}(\mathbf{x}_s) &= \dot{\mathbf{x}}_s^T \mathcal{P} \mathbf{x}_s(t) + \mathbf{x}_s^T \mathcal{P} \dot{\mathbf{x}}_s(t) \\ &= \mathbf{x}_s^T (\mathcal{P} A_{s\delta} + A_{s\delta}^T \mathcal{P}) \mathbf{x}_s(t).\end{aligned}\quad (23)$$

From the Lyapunov theorem, the closed-loop system (20) is internally asymptotically stable for all admissible uncertainties if

$$\mathcal{P} A_{s\delta} + A_{s\delta}^T \mathcal{P} < 0 \quad \forall F^T F \leq I \quad (24)$$

is satisfied.

Manipulating (24) using Lemma 1 for some scalars  $\sigma > 0$ ,  $\varphi > 0$  yields:

$$\begin{aligned}A_{so} &= \begin{bmatrix} A + BD_c C & BC_c \\ B_c C & A_c \end{bmatrix} \\ \tilde{E}_a &= \begin{bmatrix} E_a \\ 0 \end{bmatrix}, \quad \tilde{E}_c = \begin{bmatrix} E_c \\ 0 \end{bmatrix} \\ \tilde{H}_a &= [ H_a \ 0 ], \quad \hat{H}_a = H_a [ D_c C \ C_c ] \\ \Pi_o &= \mathcal{P} A_{so} + A_{so}^T \mathcal{P} \\ \tilde{\Pi} &= \begin{bmatrix} \Pi_o & \mathcal{P} \tilde{E}_a & \mathcal{P} \tilde{E}_c & \sigma \tilde{H}_a^T & \varphi \tilde{H}_a^T \\ * & -\sigma I & 0 & 0 & 0 \\ * & * & -\varphi I & 0 & 0 \\ * & * & * & -\sigma I & 0 \\ * & * & * & * & -\varphi I \end{bmatrix} \leq 0.\end{aligned}\quad (25)$$

*Remark 2:* It must be noted that checking the feasibility of (24) over  $\mathcal{P} > 0$ , the closed-loop system is stabilized. We note that the matrix inequality in (24) cannot be directly solved using LMI tools to find the controller  $\mathcal{K}$  because it is not affine in the controller parameters  $A_c$ ,  $B_c$ ,  $C_c$  and  $D_c$ .

To determine the parameters of the controller parameters  $A_c$ ,  $B_c$ ,  $C_c$  and  $D_c$ , we consider one of the following two optimization problems [21]:

1) The  $H_2$ -norm optimization in which it is required to find a controller of class (19) that ensures the stability of closed-loop system (20) and keeps the  $H_2$ -norm of the transfer function  $H_{zw}(s)$  from  $w$  to  $z$  as small as possible.

2) The  $H_\infty$ -norm optimization in which it is required to find a controller of class (19) that ensures the stability of closed-loop system (20) and keeps the  $\|z\|_2 < \gamma \|w\|_2$  for a prescribed attenuation level  $\gamma > 0$ . The objective of this paper is to develop LMI-based characterization of the two optimization problems.

### A. $H_2$ Design

Provided matrix  $A_{s\delta}$  is Hurwitz for all admissible uncertainties  $F^T F < I$ , given  $\mathcal{K}$ , as expressed by (24), and  $\Phi \equiv 0$ ,  $\Psi \equiv 0$ , the square of the  $H_2$ -norm of the transfer function  $H_{zw}(s)$  can be expressed in terms of the solution of a Lyapunov equation (controllability Grammian) such that the corresponding minimization problem with respect to the quadruple of controller parameters  $(A_c, B_c, C_c, D_c)$  is given by

$$\min \left\{ \text{Tr} [C_s^T \mathcal{P}_s C_s] : A_{s\delta} \mathcal{P}_s + \mathcal{P}_s A_{s\delta}^T + B_{s\delta} B_{s\delta}^T = 0 \right. \\ \left. \forall F^T F < I \right\} \quad (26)$$

where  $\text{Tr} [\cdot]$  denotes the trace operator. Since  $\mathcal{P}_s < \mathcal{P}$  for any  $\mathcal{P}$  satisfying

$$\mathcal{P}_{s\delta} \mathcal{P} + \mathcal{P} A_{s\delta}^T + B_{s\delta} B_{s\delta}^T < 0 \quad \forall F^T F < I \quad (27)$$

it is readily verified that  $\|H_{zw}(s)\|_2^2 = \text{Tr} [C_s^T \mathcal{P} C_s] < \nu$  for all admissible uncertainties such that  $F^T F \leq I$  if and only if there exists  $\mathcal{P} > 0$  satisfying (27) and  $\text{Tr} [B_s^T \mathcal{P} B_s] < \nu$ .

Introducing an auxiliary parameter  $\mathcal{W}$ , the following analysis result is obtained:

*Theorem 3:* Matrix  $A_s$  is stable for all admissible uncertainties such that  $F^T F \leq I$  and  $\|H_{zw}(s)\|_2^2 < \nu$  for a prescribed  $\nu$  if and only if there exist matrices  $\mathcal{P} = \widehat{\mathcal{P}}^{-1}$  and  $\mathcal{W}$  such that

$$\text{Tr} (\mathcal{W}) < \nu \quad (28)$$

$$\begin{bmatrix} A_{s\delta}^T \widehat{\mathcal{P}} + \widehat{\mathcal{P}} A_{s\delta} & \widehat{\mathcal{P}} B_{s\delta} \\ * & -I \end{bmatrix} < 0 \quad (29)$$

Now, proceeding further and in view of Remark 2, a variable transformation is necessary. By partitioning  $\widehat{\mathcal{P}}$  and  $\widehat{\mathcal{P}}^{-1}$  as

$$\widehat{\mathcal{P}} = \begin{bmatrix} \mathcal{Y} & \mathcal{N} \\ * & \widehat{\mathcal{Y}} \end{bmatrix}, \quad \widehat{\mathcal{P}}^{-1} = \begin{bmatrix} \mathcal{X} & \mathcal{M} \\ * & \widehat{\mathcal{X}} \end{bmatrix} \quad (30)$$

where  $0 < \mathcal{Y} = \mathcal{Y}^T$ ,  $0 < \mathcal{X} = \mathcal{X}^T$ , we infer

$$\widehat{\mathcal{P}} \begin{bmatrix} \mathcal{X} \\ \mathcal{M}^T \end{bmatrix} = \begin{bmatrix} I \\ 0 \end{bmatrix} \quad (31)$$

which leads to

$$\begin{aligned}\widehat{\mathcal{P}} \Xi_o &= \Xi_a \\ \Xi_a &= \begin{bmatrix} I & \mathcal{Y} \\ 0 & \mathcal{M}^T \end{bmatrix}, \quad \Xi_o = \begin{bmatrix} \mathcal{X} & I \\ \mathcal{M}^T & 0 \end{bmatrix}.\end{aligned}\quad (32)$$

Define

$$\begin{aligned}\tilde{H}_a &= [ H_a^T \ 0 \ 0 ]^T \\ \tilde{E}_a &= H_a [ 0 \ E_a \ 0 ] \\ \tilde{E}_c &= E_c [ 0 \ D_c C \ D_c \Psi ] \\ \Theta &= [ \tilde{H}_a \ \tilde{H}_a \ \sigma \tilde{E}_a^T \ \varphi \tilde{E}_a^T ] \\ \Upsilon &= \text{diag} [ \sigma I \ \varphi \ \sigma I \ \varphi ].\end{aligned}\quad (33)$$

The main design result is summarized by the following theorem:

*Theorem 4:* System (3) with controller (19) is stable with  $\|H_{zw}(s)\|_2^2 < \nu$  for a prescribed  $\nu$  if and only if there exist matrices  $0 < \mathcal{X}$ ,  $0 < \mathcal{Y}$ ,  $\Omega$ ,  $\Lambda$ ,  $\Delta$ ,  $D_c$  and  $\mathcal{W}$  such that

$$\text{Tr} (\mathcal{W}) < \nu \quad (34)$$

$$\begin{bmatrix} \Pi_o & \Omega^T + A + BD_c C & \Gamma + BD_c \Psi & \Theta \\ * & \Pi_a & \mathcal{Y} \Gamma + \Lambda \Psi & 0 \\ * & * & -I & 0 \\ * & * & * & -\Upsilon \end{bmatrix} < 0 \quad (35)$$

$$\begin{bmatrix} \mathcal{X} & I & \mathcal{X} G^T + \mathcal{C}^T D^T \\ * & \mathcal{Y} & G^T + C^T D_c^T D^T \\ * & * & \mathcal{W} \end{bmatrix} > 0 \quad (36)$$

where

$$\begin{aligned}\Pi_o &= A\mathcal{X} + \mathcal{X}A^T + B\Delta + \Delta^T B^T \\ \Pi_a &= A^T \mathcal{Y} + \mathcal{Y}A + \Lambda C + C^T \Lambda^T \\ \mathcal{M}\mathcal{N}^T &= I - \mathcal{X}\mathcal{Y}.\end{aligned}\quad (37)$$

Moreover, the controller gains are given by

$$\begin{aligned}C_c &= [\Delta - D_c C \mathcal{X}] \mathcal{M}^{-T} \\ B_c &= [\Lambda - \mathcal{Y} B D_c] \mathcal{N}^{-1} \\ A_c &= \mathcal{N}^{-1} [\Omega - \mathcal{N} B_c C \mathcal{X} + \mathcal{Y} B C_c \mathcal{M}^T \\ &\quad - \mathcal{Y}(A + B D_c C) \mathcal{X}] \mathcal{M}^{-T}.\end{aligned}\quad (38)$$

*Proof:* The theorem can be established in three-steps. First, we perform a congruence transformation with  $\text{diag}[\Xi_o, I]$  on both inequalities (29). Second, we use the following relations

$$\begin{aligned}\Xi_o^T \widehat{\mathcal{P}} A_{s\delta} \Xi_o &= \begin{bmatrix} A\delta\mathcal{X} + B\delta\Delta & A\delta + B\delta D_c C \\ \Omega & \mathcal{Y}A\delta + \Lambda C \end{bmatrix} \\ &\quad + \mathcal{Y}(A_\delta + B_\delta D_c C)\mathcal{X} \\ \Xi_o^T \widehat{\mathcal{P}} B_{s\delta} &= \begin{bmatrix} \Gamma + B_\delta D_c \Psi \\ \mathcal{Y}\Gamma + \Lambda\Psi \end{bmatrix} \\ C_s \Xi_o &= \begin{bmatrix} G\mathcal{X} + D\Delta & G + DD_c C \end{bmatrix} \\ \Xi_o^T \widehat{\mathcal{P}} \Xi_o &= \begin{bmatrix} \mathcal{X} & I \\ * & \mathcal{Y} \end{bmatrix}.\end{aligned}\quad (39)$$

Third, we introduce the change of controller variables:

$$\begin{aligned}\Omega &= \mathcal{N} A_c \mathcal{M}^T + \mathcal{N} B_c C \mathcal{X} + \mathcal{Y} B C_c \mathcal{M}^T \\ &\quad + \mathcal{Y}(A + B D_c C)\mathcal{X}\end{aligned}\quad (40)$$

$$\Lambda = \mathcal{N} B_c + \mathcal{Y} B D_c \quad (41)$$

$$\Delta = C_c \mathcal{M}^T + D_c C \mathcal{X}. \quad (42)$$

Then, by algebraic manipulations using (30), invoking Lemma (1) and the fact  $\widehat{\mathcal{P}} \widehat{\mathcal{P}}^{-1} = I$ , we obtain LMIs (35)–(36). The controller gains (38) are derived by reversing relations (40)–(42). ■

In the case of strictly proper controllers

$$\begin{aligned}\dot{\mathbf{x}}_c(t) &= A_c \mathbf{x}_c(t) + B_c \mathbf{y}(t) \\ \mathbf{u}(t) &= C_c \mathbf{x}_c(t)\end{aligned}\quad (43)$$

we obtain the following design result.

*Corollary 1:* System (3) with controller (43) is stable with  $\|H_{zw}(s)\|_2^2 < \nu$  for a prescribed  $\nu$  if and only if there exist matrices  $0 < \mathcal{X}$ ,  $0 < \mathcal{Y}$ ,  $\Omega$ ,  $B$ ,  $C$  and  $\mathcal{W}$  such that

$$\text{Tr}(\mathcal{W}) < \nu \quad (44)$$

$$\begin{bmatrix} \Pi_o & \Omega^T + A & \Gamma \\ * & \Pi_a & \mathcal{Y}\Gamma + \Lambda\Psi \\ * & * & -I \end{bmatrix} < 0 \quad (45)$$

$$\begin{bmatrix} \mathcal{X} & I & \mathcal{X}G^T + \Delta^T D^T \\ * & \mathcal{Y} & G^T \\ * & * & \mathcal{W} \end{bmatrix} > 0 \quad (46)$$

where

$$\begin{aligned}\Pi_o &= A\mathcal{X} + \mathcal{X}A^T + B\Delta + \Delta^T B^T \\ \Pi_a &= A^T \mathcal{Y} + \mathcal{Y}A + \Lambda C + C^T \Lambda^T \\ \mathcal{M}\mathcal{N}^T &= I - \mathcal{X}\mathcal{Y}.\end{aligned}\quad (47)$$

Moreover, the controller gains are given by

$$\begin{aligned}C_c &= \Delta \mathcal{M}^{-T} \\ B_c &= \Lambda \mathcal{N}^{-1} \\ A_c &= \mathcal{N}^{-1} [\Omega - \mathcal{N} B_c C \mathcal{X} + \mathcal{Y} B C_c \mathcal{M}^T \\ &\quad - \mathcal{Y} A \mathcal{X}] \mathcal{M}^{-T}.\end{aligned}\quad (48)$$

*Proof:* Follows from Theorem 4 by setting  $D_c \equiv 0$ . ■

### B. $H_\infty$ Design

In what follows, we consider the  $H_\infty$ -norm optimization problem. It follows from robust control theory [21] that the solution of this problem corresponds to determining the controller parameters that guarantee the feasibility of

$$\dot{V}(\mathbf{x}_s) + \mathbf{z}^T(t) \mathbf{z}(t) - \gamma^2 \mathbf{w}^T(t) \mathbf{w}(t) < 0. \quad (49)$$

The design result is summarized by the following theorem:

*Theorem 5:* System (26) is asymptotically stable with  $\gamma$ -disturbance attenuation if there exist matrices  $0 < \mathcal{X}$ ,  $0 < \mathcal{Y}$ ,  $\Omega$ ,  $\Lambda$ ,  $\Delta$ ,  $D_c$  satisfying the following LMI

$$\begin{bmatrix} \Pi_o & \Omega^T + A + B D_c C & \Gamma + B D_c \Psi & \mathcal{X} G^T + \Delta^T D^T \\ * & \Pi_a & \mathcal{Y}\Gamma + \Lambda\Psi & G^T + C^T D_c^T D^T \\ * & * & -\gamma^2 I & \Phi^T + \Psi^T D_c^T D^T \\ * & * & * & -I \end{bmatrix} < 0 \quad (50)$$

where

$$\begin{aligned}\Pi_o &= A\mathcal{X} + \mathcal{X}A^T + B\Delta + \Delta^T B^T \\ \Pi_a &= A^T \mathcal{Y} + \mathcal{Y}A + \Lambda C + C^T \Lambda^T \\ \mathcal{M}\mathcal{N}^T &= I - \mathcal{X}\mathcal{Y}.\end{aligned}\quad (51)$$

Moreover, the controller gains are given by

$$\begin{aligned}C_c &= [\Delta - D_c C \mathcal{X}] \mathcal{M}^{-T} \\ B_c &= [\Lambda - \mathcal{Y} B D_c] \mathcal{N}^{-1} \\ A_c &= \mathcal{N}^{-1} [\Omega - \mathcal{N} B_c C \mathcal{X} + \mathcal{Y} B C_c \mathcal{M}^T \\ &\quad - \mathcal{Y}(A + B D_c C) \mathcal{X}] \mathcal{M}^{-T}.\end{aligned}\quad (52)$$

*Proof:* With the aid of (23), we express inequality (49) in the form

$$\begin{aligned}\mathbf{x}_s^T [\mathcal{P} A_s + A_s^T \mathcal{P}] \mathbf{x}_s + [C_s \mathbf{x}_s + D_s \mathbf{w}]^T [C_s \mathbf{x}_s + D_s \mathbf{w}] \\ + 2\mathbf{x}^T \mathcal{P} B_s - \gamma^2 \mathbf{w}^T \mathbf{w} < 0\end{aligned}\quad (53)$$

Inequality (53), by Schur complement, is equivalent to

$$\begin{bmatrix} \mathcal{P} A_s + A_s^T \mathcal{P} & \mathcal{P} B_s & C_s^T \\ * & -\gamma^2 I & D_s^T \\ * & * & -I \end{bmatrix} < 0 \quad (54)$$

for any  $[\mathbf{x}_s, \mathbf{w}] \neq 0$ . Applying the congruent transformation  $\text{diag}[\Xi_o, I, I]$  to (54) and making use of expressions (39)–(42) with  $\mathcal{P} \leftarrow \widehat{\mathcal{P}}$ , we readily obtain LMI (50) subject to (51). The controller gains (38) are derived by reversing relations (40)–(42), which concludes the proof. ■

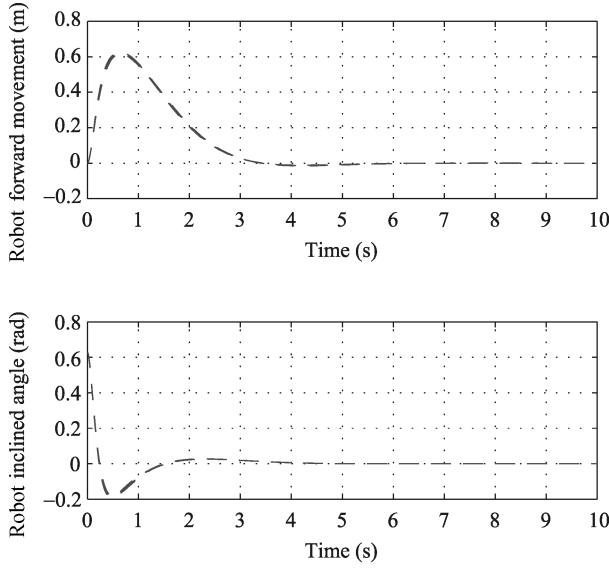


Fig. 4. Closed-loop system response using LQR controller.

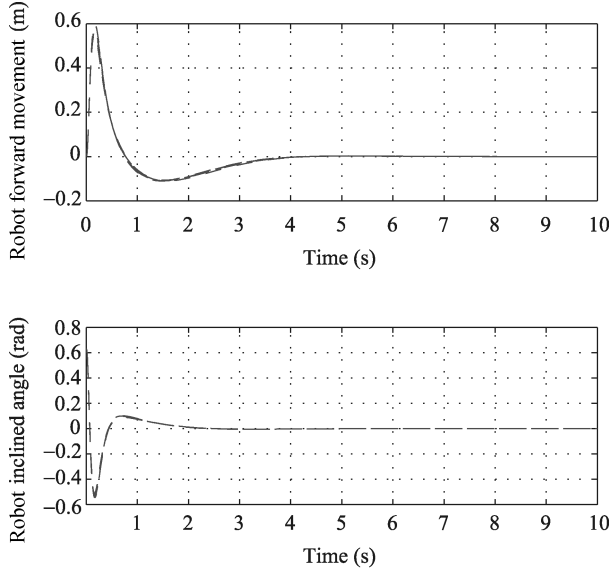


Fig. 5. Closed-loop system response using LQG controller.

## V. SIMULATION RESULTS

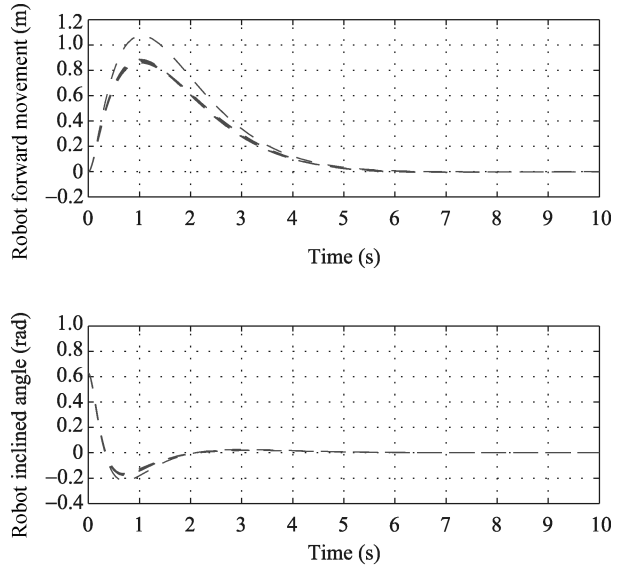
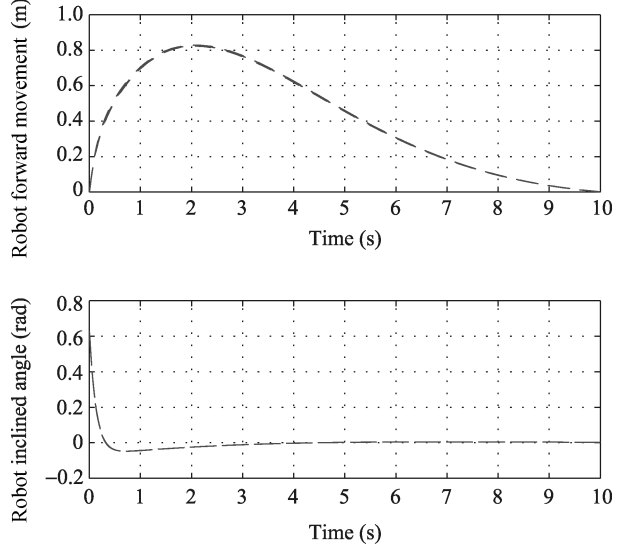
Several simulation experiments of balancing, linear running, and steering have been carried out using the stabilization methods of  $LQR$ ,  $LQG$ ,  $H_2$  and  $H_\infty$ . Two sets of experiments were performed:

*Set A:* Nominal model in which the parametric uncertainties are suppressed  $\delta A \equiv 0$ ,  $\delta B \equiv 0$ .

*Set B:* Uncertain model in which the parametric uncertainties are added to the mass and inertia of the robot  $\pm 10\%$  of their nominal values.

### A. Results of Nominal Model

Using the nominal model, the ensuing results are depicted in Figs. 4–7 for the two output variables: the robot forward movement and the robot inclination angle. In Fig. 8, a comparison among the design methods is presented.

Fig. 6. Closed-loop system response using  $H_2$  controller.Fig. 7. Closed-loop system response using  $H_\infty$  controller.

### B. Case of Modeling Errors

It follows from Theorem 4 that system (3) with controller (19) is stable with  $\|H_{zw}(s)\|_2^2 < \nu$  for a prescribed  $\nu$  if and only if there exist matrices  $0 < \mathcal{X}$ ,  $0 < \mathcal{Y}$ ,  $\Omega$ ,  $\Lambda$ ,  $\Delta$ ,  $D_c$  and  $\mathcal{W}$  such that the following LMIs hold for all admissible uncertainties satisfying (4)

$$\text{Tr}(\mathcal{W}) < \nu \quad (55)$$

$$\begin{bmatrix} \Pi_{o\delta} & \Omega^T + A_\delta + B_\delta D_c C & \Gamma + A_\delta D_c \Psi \\ * & \Pi_{a\delta} & \mathcal{Y}\Gamma + \Lambda\Psi \\ * & * & -I \end{bmatrix} < 0 \quad (56)$$

$$\begin{bmatrix} \mathcal{X} & I & \mathcal{X}G^T + \Delta^T D^T \\ * & \mathcal{Y} & G^T + C^T D_c^T D^T \\ * & * & \mathcal{W} \end{bmatrix} > 0 \quad (57)$$

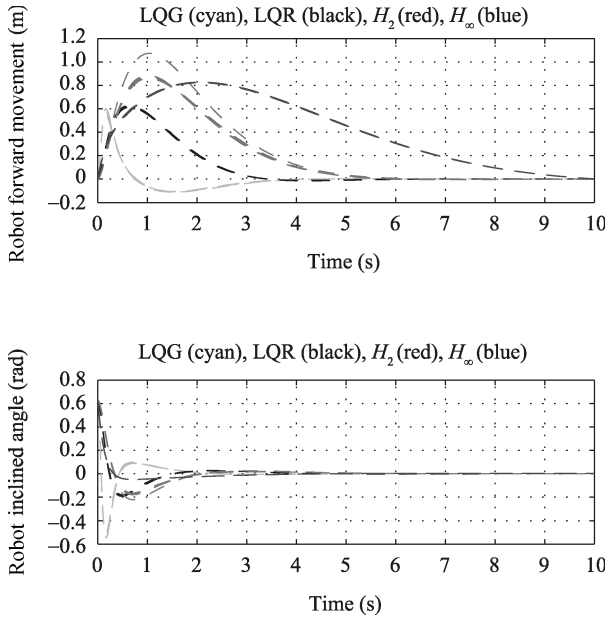


Fig. 8. Comparison of output trajectories-nominal case.

where

$$\begin{aligned}\Pi_{o\delta} &= A_\delta \mathcal{X} + \mathcal{X} A_\delta^T + B_\delta \Delta + \Delta^T B_\delta^T \\ \Pi_{a\delta} &= A_\delta^T \mathcal{Y} + \mathcal{Y} A_\delta + \Lambda C + C^T \Lambda^T \\ \mathcal{M}\mathcal{N}^T &= I - \mathcal{X}\mathcal{Y}.\end{aligned}\quad (58)$$

By applying a convex analysis procedure in the manner of [22]–[24], the corresponding robust  $H_2$  design results are summarized by the following theorem:

**Theorem 6:** System (3) with controller (19) is robustly asymptotically stable with  $\|H_{zw}(s)\|_2^2 < \nu$  for a prescribed  $\nu$  if there exist matrices  $0 < \mathcal{X}, 0 < \mathcal{Y}, \Omega, \Lambda, \Delta, D_c, \mathcal{W}$  and scalar parameters  $\varepsilon_a > 0, \varepsilon_c > 0$ , such that

$$\text{Tr}(\mathcal{W}) < \nu \quad (59)$$

$$\left[ \begin{array}{cccc} \Pi_o & \Omega^T + A + BD_cC & \Gamma + BD_c\Psi & \mathcal{X}E_a^T \\ * & \Pi_a & \mathcal{Y}\Gamma + \Lambda\Psi & \\ * & * & -I & \\ * & * & * & \\ * & * & * & \\ * & * & * & \\ \varepsilon_a H_a & \mathcal{X}E_a^T & 0 & 0 \\ 0 & E_a^T + C^T D_c^T E_c^T & \mathcal{Y}H_a & \varepsilon_c E_a^T \\ 0 & \Psi^T D_c^T E_a^T & 0 & 0 \\ -\varepsilon_a I & 0 & 0 & 0 \\ * & -\varepsilon_a I & 0 & 0 \\ * & * & -\varepsilon_c I & 0 \\ * & * & * & -\varepsilon_c I \end{array} \right] < 0 \quad (60)$$

$$\left[ \begin{array}{ccc} \mathcal{X} & I & \mathcal{X}G^T + C^T D^T \\ * & \mathcal{Y} & G^T + C^T D_c^T D^T \\ * & * & \mathcal{W} \end{array} \right] > 0 \quad (61)$$

where  $\Pi_o, \Pi_a, \mathcal{M}\mathcal{N}^T$  are given by (37). Moreover, the controller gains are given by (38).

In a similar way, the corresponding robust result of the  $H_\infty$ -norm optimization problem is cast into the following theorem:

**Theorem 7:** System (3) with controller (19) is robustly asymptotically stable with  $\gamma$ -disturbance attenuation if there exist matrices  $0 < \mathcal{X}, 0 < \mathcal{Y}, \Omega, \Lambda, \Delta, D_c$  satisfying the following LMI

$$\left[ \begin{array}{ccccc} \Pi_o & \Omega^T + A + BD_cC & \Gamma + BD_c\Psi & \mathcal{X}G^T + \Delta^T D^T \\ * & \Pi_a & \mathcal{Y}\Gamma + \Lambda\Psi & G^T + C^T D_c^T D^T \\ * & * & -\gamma^2 I & \Phi^T + \Psi^T D_c^T D^T \\ * & * & * & -I \\ * & * & * & * \\ * & * & * & * \\ * & * & * & * \\ * & * & * & * \\ \varepsilon_a H_a & \mathcal{X}E_a^T & 0 & 0 \\ 0 & E_a^T + C^T D_c^T E_c^T & \mathcal{Y}H_a & \varepsilon_c E_a^T \\ 0 & \Psi^T D_c^T E_a^T & 0 & 0 \\ 0 & 0 & 0 & 0 \\ -\varepsilon_a I & 0 & 0 & 0 \\ * & -\varepsilon_a I & 0 & 0 \\ * & * & -\varepsilon_c I & 0 \\ * & * & * & -\varepsilon_c I \end{array} \right] < 0 \quad (62)$$

where  $\Pi_o, \Pi_a, \mathcal{M}\mathcal{N}^T$  are given by (37). Moreover, the controller gains are given by (38).

### C. Results of Uncertain Model

Using the uncertain model, the ensuing results are depicted in Figs. 9–12 for the two output variables: the robot forward movement and the robot inclination angle. In Fig. 13, a comparison among the design methods is presented.

From the simulation results, we can arrive at the following points:

- 1) Smooth behavior is clearly demonstrated for the patterns of the output variables;

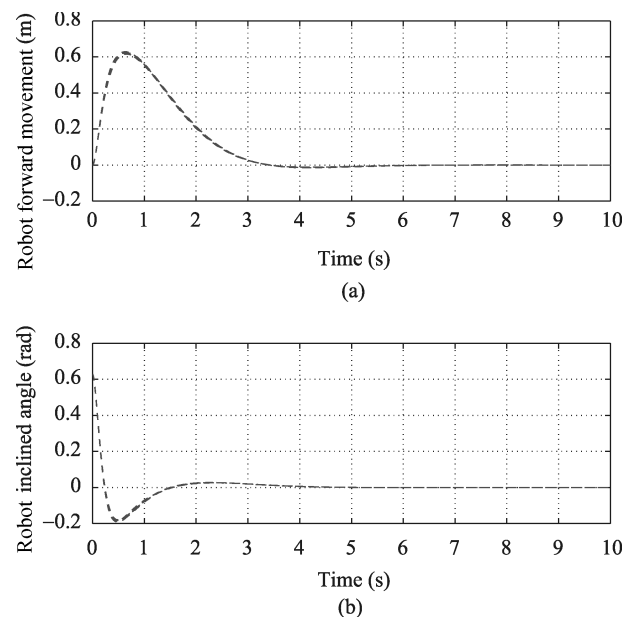


Fig. 9. Closed-loop response using LQR controller.

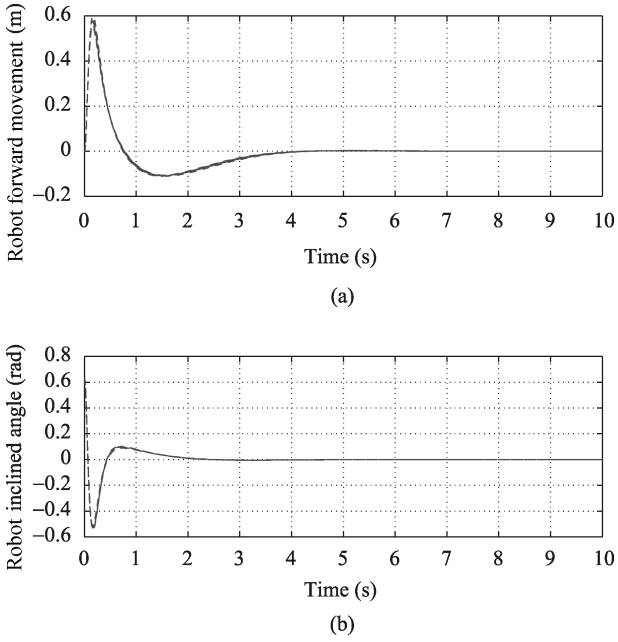
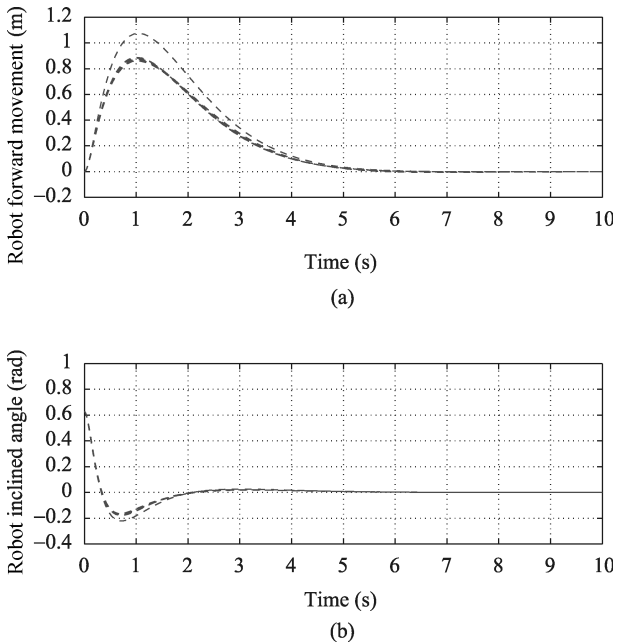


Fig. 10. Closed-loop response using LQG controller.

Fig. 11. Closed-loop response using  $H_2$  controller.

- 2) The LQR design determines one gain matrix for the feedback control while the LQG design determines two gain matrices: one for the control and the other for the estimator;
- 3) In terms of the dynamic feedback control, three gain matrices are obtained based on the design methods of  $H_2$  and  $H_\infty$ .

## VI. EXPERIMENTAL RESULTS FOR UPRIGHT BALANCING

Using the lab capabilities at King Fahd University of Petroleum and Minerals (KFUPM), Fig. 14 illustrates two-wheeled inverted pendulum robot experiment. It consists of two motor drives, two motors, a 32-bit microcontroller, an inertial measurement unit (IMU), and two encoders. 3-axis gyro sensor and 3-axis accelerometer are installed in IMU

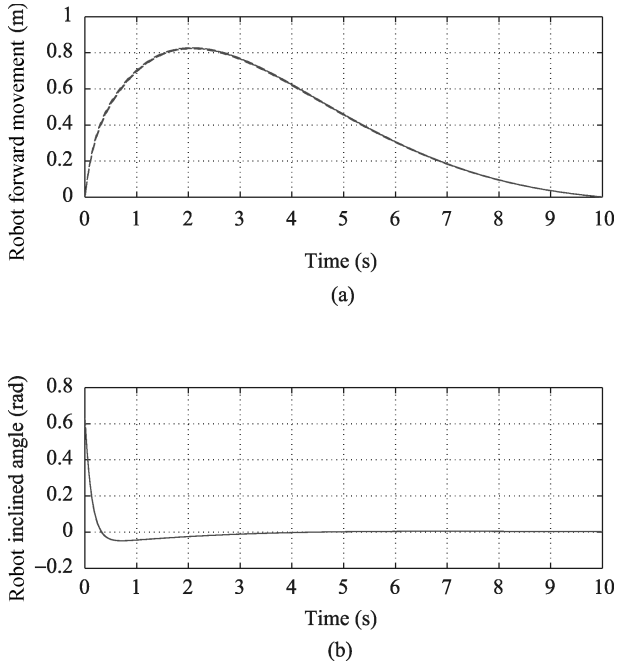
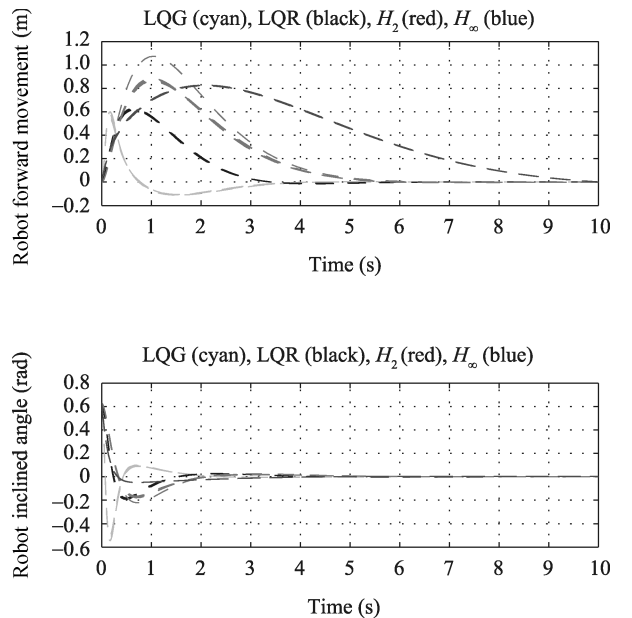
Fig. 12. Closed-loop response using  $H_\infty$  controller.

Fig. 13. Comparison of output trajectories-uncertain case.

sensor. To operate the robot as shown in Fig. 2, IMU sensor precedes the data of gyro sensor and accelerometer by Kalman filter in order to estimate the angular velocity and tilt angle of the body. The encoder is detected by the rotation of both wheels then they are converted to position and velocity in Cartesian coordinate frame. Then, position, velocity, yaw angle, yaw rate, tilt angle, pitch rate are used to compute the control law. It will send the command to motor drivers in order that the motor drivers produce electronic current and voltage for motors.

Stable upright balancing is crucial for controlling the inverted pendulum robots, particularly in the absence of bearing between the base and the upper body of the two-wheeled robot.

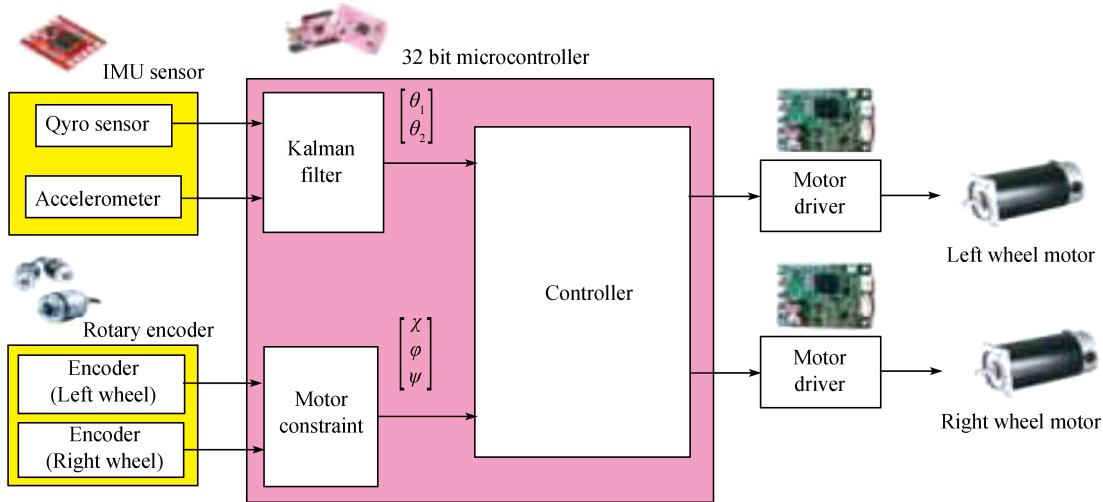


Fig. 14. Two-wheeled inverted pendulum robot experiment.

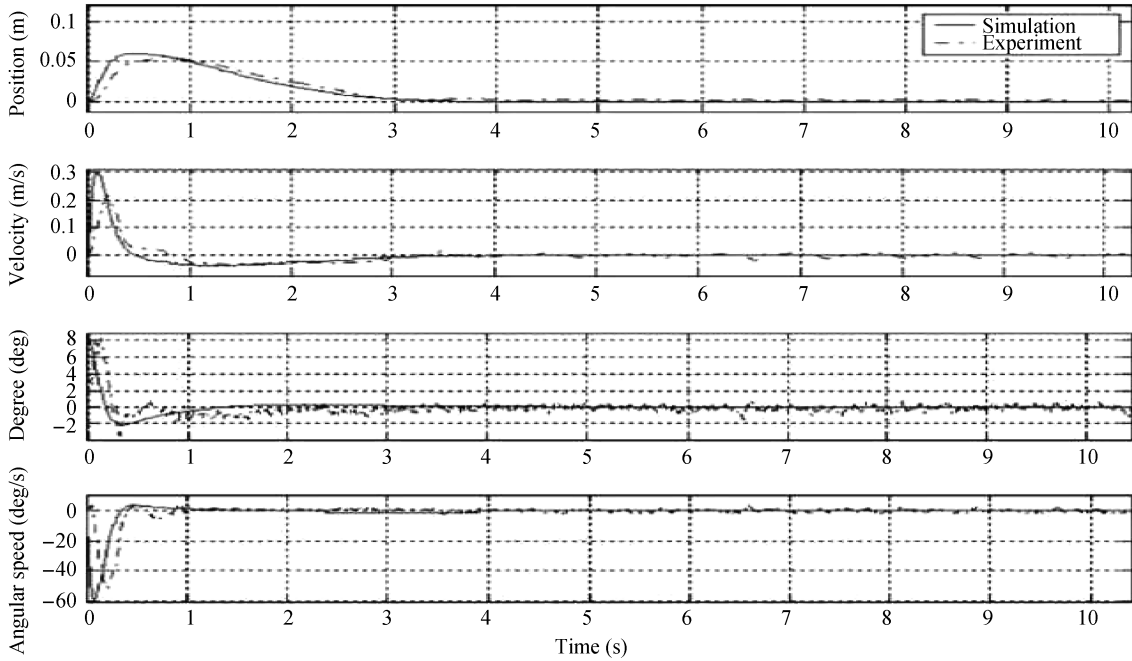


Fig. 15. Upright balancing: experimental results.

We have applied the  $H_2$  control algorithm since it exhibits superior simulation results. The upper balancing enables the robot to keep its original position without losing its balance. An experiment was performed to demonstrate this feature. The robot was initially tilted  $8^\circ$  but the angular velocity of the tilt angle was zero. The ensuing graphical results are depicted in Fig. 15, from which we record that the tilt angle of the mass center of the body and its time derivative cross the horizontal axis within 0.24 s. After almost 3 s, the position of the center of the base returned to its original position.

## VII. CONCLUSIONS

In this paper, the two wheeled robot is stabilized by using four different control methods, LQR, LQG,  $H_2$  and  $H_\infty$ . The design procedure is formulated as optimization feasibility problem over LMIs. By simulation studies, their performance

are generated and compared. According to modeling set-up and subsequent simulation results, it is concluded that the  $H_\infty$  outperform the other methods. Experimental results are reported for upright balancing task.

## REFERENCES

- [1] S. Jeong and T. Takahashi, "Wheeled inverted pendulum type assistant robot: Design concept and mobile control," *Intell. Serv. Rob.*, vol. 1, no. 4, pp. 313–320, Oct. 2008.
- [2] A. Sinha, P. Prasoon, P. K. Bharadwaj, and A. C. Ranasinghe, "Nonlinear autonomous control of a two-wheeled inverted pendulum mobile robot based on sliding mode," in *Proc. Int. Conf. Computational Intelligence and Networks (CINE)*, Bhubaneswar, India, 2015, pp. 52–57.
- [3] J. Huang, S. Ri, L. Liu, Y. J. Wang, J. Kim, and G. Pak, "Nonlinear disturbance observer-based dynamic surface control of mobile wheeled inverted pendulum," *IEEE Trans. Control Syst. Technol.*, vol. 23, no. 6, pp. 2400–2407, Nov. 2015.

- [4] M. A. H. Garzón, W. O. C. Hernández, A. P. G. Reyes, and O. E. C. Quintero, “Two-wheeled inverted pendulum robot NXT Lego Mindstorms: mathematical modelling and real robot comparisons,” *Rev. Politécnica*, vol. 36, no. 1, Sep. 2015.
- [5] M. M. Azimi and H. R. Koofifar, “Model predictive control for a two wheeled self balancing robot,” in *Proc. 1st RSI/ISM Int. Conf. Robotics and Mechatronics (ICRoM)*, Tehran, Iran, 2013, pp. 152–157.
- [6] Z. J. Li, C. G. Yang, and L. P. Fan, *Advanced Control of Wheeled Inverted Pendulum Systems*. New York, London, USA: Springer, 2013.
- [7] Z. J. Li and C. Q. Xu, “Adaptive fuzzy logic control of dynamic balance and motion for wheeled inverted pendulums,” *Fuzzy Sets Syst.*, vol. 160, no. 12, pp. 1787–1803, Jun. 2009.
- [8] S. Jung and S. S. Kim, “Control experiment of a wheel-driven mobile inverted pendulum using neural network,” *IEEE Trans. Control Syst. Technol.*, vol. 16, no. 2, pp. 297–303, Mar. 2008.
- [9] J. Huang, Z. H. Guan, T. Matsuno, T. Fukuda, and K. Sekiyama, “Sliding-mode velocity control of mobile-wheeled inverted-pendulum systems,” *IEEE Trans. Robot.*, vol. 26, no. 4, pp. 750–758, Aug. 2010.
- [10] C. G. Yang, Z. J. Li, and J. Li, “Trajectory planning and optimized adaptive control for a class of wheeled inverted pendulum vehicle models,” *IEEE Trans. Cybern.*, vol. 43, no. 1, pp. 24–36, Feb. 2013.
- [11] Z. C. Li, Y. Wang, and Z. Liu, “Unscented Kalman filter-trained neural networks for slip model prediction,” *PLoS One*, vol. 11, no. 7, pp. e0158492, Jul. 2016, doi: 10.1371/journal.pone.0158492.
- [12] J. Moreno-Valenzuela, C. Aguilar-Avelar, S. Puga-Guzmán, and V. Santibáñez, “Two adaptive control strategies for trajectory tracking of the inertia wheel pendulum: neural networks vis à vis model regressor,” *Intell. Autom. Soft Comput.*, vol. 23, no. 1, pp. 63–73, Jan. 2016.
- [13] R. X. Cui, J. Guo, and Z. Y. Mao, “Adaptive backstepping control of wheeled inverted pendulums models,” *Nonlinear Dyn.*, vol. 79, no. 1, pp. 501–511, Jan. 2015.
- [14] Y. Maruki, K. Kawano, H. Suemitsu, and T. Matsuo, “Adaptive backstepping control of wheeled inverted pendulum with velocity estimator” *Int. J. Control. Autom. Syst.*, vol. 12, no. 5, pp. 1040–1048, Oct. 2014.
- [15] H. Vasudevan, A. M. Dollar, and J. B. Morrell, “Design for control of wheeled inverted pendulum platforms,” *J. Mech. Rob.*, vol. 7, no. 4, pp. 041005, Nov. 2015.
- [16] S. Jeong and T. Takahashi, “Wheeled inverted pendulum type assistant robot: Inverted mobile, standing, and sitting motions,” in *Proc. IEEE/RSJ Int. Conf. Intelligent Robots and Systems*, San Diego, CA, USA, 2007, pp. 1932–1937.
- [17] K. Pathak, J. Franch, and S. K. Agrawal, “Velocity and position control of a wheeled inverted pendulum by partial feedback linearization,” *IEEE Trans. Robot.*, vol. 21, no. 3, pp. 505–513, Jun. 2005.
- [18] “Matlab Documents,” MPC guide, *Mathworks*, USA.
- [19] B. D. O. Anderson and J. B. Moore, *Linear Optimal Control*. Englewood Cliffs, NJ, USA: Prentice-Hall, Inc., 1971.
- [20] M. S. Mahmoud and Y. Q. Xia, *Applied Control Systems Design: State-Space Methods*. London, UK: Springer-Verlag, 2012.
- [21] K. M. Zhou and J. C. Doyle, *Essentials of Robust Control*. New Jersey, USA: Prentice-Hall, 1998.
- [22] M. S. Mahmoud, *Resilient Control of Uncertain Dynamical Systems*. Berlin, Heidelberg, Germany: Springer, 2004.
- [23] M. S. Mahmoud and A. Y. Al-Rayyah, “Efficient parameterisation to stability and feedback synthesis of linear time-delay systems,” *IET Control Theory Appl.*, vol. 3, no. 8, pp. 1107–1118, Aug. 2009.
- [24] M. S. Mahmoud and Y. Q. Xia, “Robust filter design for piecewise discrete-time systems with time-varying delays,” *Int. J. Robust Nonlinear Control*, vol. 20, no. 5, pp. 544–560, Mar. 2010.



**Magdi S. Mahmoud** obtained B.Sc. (Honors) in communication engineering, M.Sc. in electronic engineering and Ph.D. in systems engineering, all from Cairo University in 1968, 1972, and 1974, respectively. He has been a Professor of engineering since 1984. He is now a Distinguished Professor at KFUPM, Saudi Arabia. He was on the faculty at different universities worldwide including Egypt (CU, AUC), Kuwait (KU), UAE (UAEU), UK (UMIST), USA (Pitt, Case Western), Singapore (Nanyang) and Australia (Adelaide). He lectured in Venezuela (Caracas), Germany (Hanover), UK (Kent), USA (UoSA), Canada (Montreal) and China (BIT, Yanshan). He is the principal author of thirty-seven books, inclusive book-chapters and the author/co-author of more than 565 peer-reviewed papers. He is a fellow of the IEEE, a senior member of the IEEE, the CEI (UK), and a registered consultant engineer of information engineering and systems (Egypt). He received the Science State Incentive Prize for outstanding research in engineering (1978, 1986), the State Medal for Science and Art, First Class (1978), and the State Distinction Award (1986), Egypt. He was awarded the Abdulhamed Showman Prize for Young Arab Scientists in the field of Engineering Sciences (1986), Jordan. In 1992, he received the Distinguished Engineering Research AWARD, College of Engineering and Petroleum, Kuwait University (1992), Kuwait.

He is co-winner of the Most Cited Paper Award 2009, *Signal Processing*, vol. 86, no. 1, 2006, pp. 140–152. His papers were selected among the 40 best papers in electrical & electronic engineering by the Web of Science ISI in July 2012. He was interviewed for “People in Control”, IEEE Control Systems Magazine, August 2010. He served as Guest Editor for the special issue *Neural Networks and Intelligent Systems in Neurocomputing* and Guest Editor for the 2015 International Symposium on Web of Things and Big Data (WoTBD 2015), 18–20 October, 2015, Manama, Bahrain.

He is a Regional Editor (Middle East and Africa) of *International Journal of Systems, Control and Communications (JSCC)*, Inderscience Publishers since 2007, member of the editorial board of the *Journal of Numerical Algebra, Control and Optimization (NACO)*, Australia, since 2010, an Associate Editor of the *International Journal of Systems Dynamics Applications (IJSDA)*, since 2011, member of the editorial board of the *Journal of Engineering Management*, USA, since 2012 and an Academic Member of Athens Institute for Education and Research, Greece, since 2015. Since 2016, he is an Editor of the *Journal Mathematical Problems in Engineering*, Hindawi Publishing Company, USA.

He is currently actively engaged in teaching and research in the development of modern methodologies to distributed control and filtering, networked-control systems, triggering mechanisms in dynamical systems, fault-tolerant systems and information technology.



**Mohamed T. Nasir** is a Ph.D. candidate in control and system engineering at King Fahd University of Petroleum & Minerals. He finished his master degree from Jordan University of Science and Technology in mechatronics engineering, and his bachelor degree from the University of Jordan. His current interests include robotics and control system design.